

## Q23 Supporting Information

# Hydantoin Hexameric Rosettes: Harnessing H-Bonds for Supergelation and Liquid Crystals

*Lucía González<sup>a</sup>, Iván Marín<sup>a</sup>, Rosa M. Tejedor<sup>b</sup>, Joaquín Barberá<sup>a</sup>, Pilar Romero<sup>a</sup>, Alberto Concellón<sup>a</sup>, Santiago Uriel<sup>\*,a</sup>, and José L. Serrano<sup>\*,a</sup>*

<sup>a</sup> Departamento de Química Orgánica, Instituto de Nanociencia y Materiales de Aragón (INMA), CSIC-Universidad de Zaragoza, 50010, Zaragoza, Spain.

<sup>b</sup> Centro Universitario de la Defensa, Academia General Militar, Zaragoza, Spain

# CONTENTS

## **1. Materials and techniques**

1.1. Materials

1.2. Techniques

## **2. Synthetic Procedures**

2.1. Synthesis of 8-(4-hydroxyphenyl)-1,3-diazaspiro[4.5]decane-2,4-dione. ((**Z**)-**2** and (**E**)-**2**)

2.2. Synthesis of 3,4,5-tris(decyloxy)benzoic anhydride. (**3**)

2.3. Synthesis of 4-(2,4-dioxo-1,3-diazaspiro[4.5]decan-8-yl)phenyl-3,4,5-tris(decyloxy)benzoate. ((**Z**)-**4** and (**E**)-**4**)

## **3. Supplementary figures**

3.1. NMR Spectra

3.2 Quantitative DOSY analysis of diastereomer (**Z**)-**4**

3.3. XRD

3.4. DSC Traces and POM images

3.5. TEM and SEM images

## **4. Theoretical calculation**

4.1. Computational details

4.2. Results

## **5. References**

# 1. MATERIALS AND CHARACTERIZATION TECHNIQUES

## 1.1 Materials

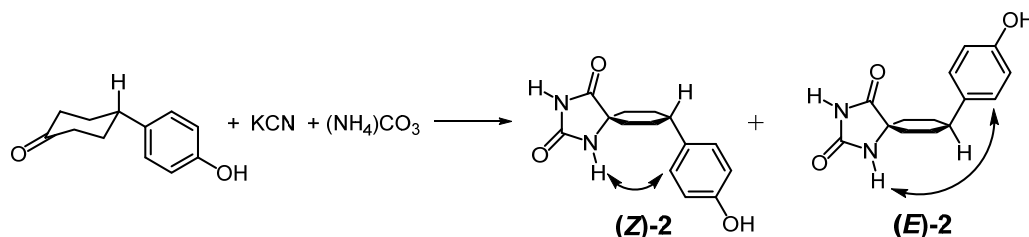
All commercially available reagents were purchased and used without further purification. Reactions were monitored by thin-layer chromatography (TLC) analysis on Merck silica gel 60 F254 TLC plates, using visualization by UV irradiation. Column chromatographic separations were performed using Merck 60 silica gel (40-63 $\mu$ m) and, unless otherwise stated, the samples were loaded as solutions in the eluent.

## 1.2 Instruments

FT-IR spectra were recorded on a Nicolet Avatar FTIR spectrometer using KBr pellets. Nuclear magnetic resonance (NMR) spectra were recorded on Bruker Avance 400 spectrometer (9.4T, 400.13 MHz for  $^1\text{H}$ , 100.62 MHz for  $^{13}\text{C}$ )  $^1\text{H}$  and  $^{13}\text{C}$  chemical shifts ( $\delta$ ) are reported in ppm relative to tetramethylsilane, using solvent residual signals as the reference.  $^1\text{H}$  NMR diffusion measurements were performed by using the bipolar-gradient LED (BPLED) pulse sequence. The diffusion time ( $\Delta$ ) was set between 120-200 ms, the pulsed gradients were incremented from 2 to 95% of the maximum strength in sixteen spaced steps with a duration ( $\delta/2$ ) of 1.1 to 1.6 ms and a LED delay of 5 ms. The diffusion coefficients,  $D$ , have been determined for all the compounds according to the equation  $I = I_0 \exp[-D\gamma^2 G^2 \delta(\Delta - \delta/3 - \tau/2)]$ , where  $I$  is the observed intensity;  $I_0$ , the reference intensity;  $G$ , the gradient amplitude;  $\delta$ , the duration of the gradient;  $\gamma$ , the gyromagnetic ratio;  $\Delta$ , the diffusion time and  $\tau$  the LED delay of 5 ms. We chose tetramethylsilane (TMS) and tetakis(trimethylsilyl)silane as internal references. MS-Maldi spectra were obtained on a MICROFLEX (Bruker Daltonics) spectrometer and MS-ESI spectra were obtained on an ESQUIRE 3000plus (Bruker Daltonics) spectrometer. The mesophase identification was based on microscopic examination of the textures formed by samples between two glass plates. NIKON and OLYMPUS BH-2 polarizing microscopes equipped with a LINKAM THMS600 hot stage were used. The temperatures and enthalpies of the phase transitions were determined by calorimetric measurements performed with DSC TA Instrument Q-20 and Q-2000 systems. Thermogravimetric analysis (TGA) was performed using a TA Q5000IR instrument at a heating rate of 10  $^\circ\text{C}$  /min under a nitrogen atmosphere. The X-ray investigations on non-oriented samples were carried out in Lindemann capillary tubes (diameter: 0.9 or 1 mm) using a PINHOLE (ANTON-PAAR) film camera operating with a point-focused Ni-filtered Cu-K $\alpha$  beam.

## 2. Synthetic procedures

### 2.1 Synthesis of 8-(4-hydroxyphenyl)-1,3-diazaspiro[4.5]decane-2,4-dione ((**Z**)-**2** and (**E**)-**2**)

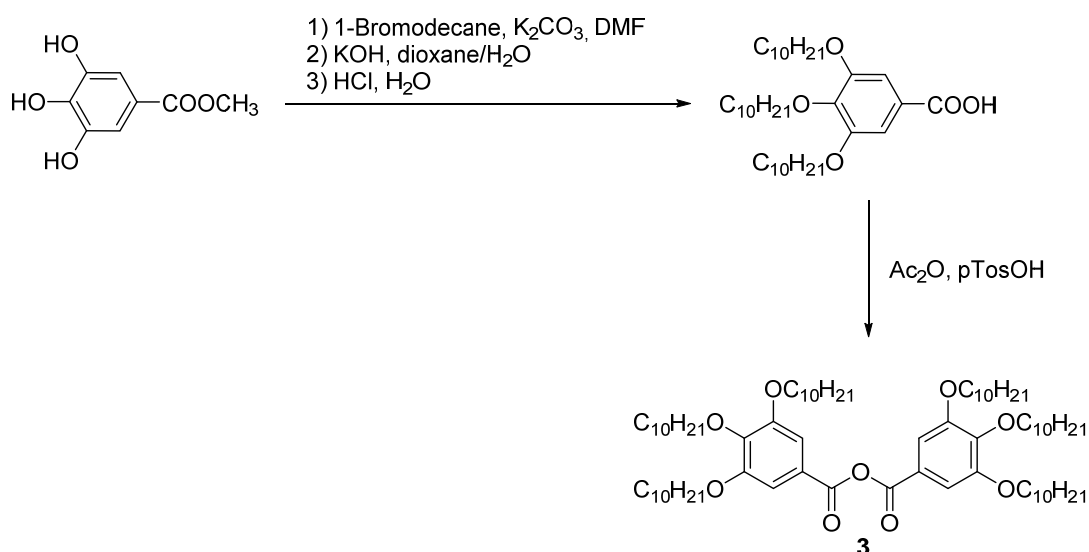


**Scheme S1**

8-(4-Hydroxyphenyl)-1,3-diazaspiro[4.5]decane-2,4-dione was synthesized by a modification of literature procedure.<sup>1</sup> A mixture of 4-(4-hydroxyphenyl)-cyclohexanone (1.33 mmol), KCN (2.65 mmol) and (NH<sub>4</sub>)<sub>2</sub>CO<sub>3</sub> (7.86 mmol) were mixed in ethanol/water (3/2) (20 mL) and the mixture was loaded into a Teflon-lined stainless steel autoclave. The sealed autoclave was heated under autogenous pressure at 100 °C overnight. The resulting mixture was cooled to ambient temperature and the precipitate was filtered off, washed with ice-cold water and ethanol. Afterwards it was dried to yield a mixture of *cis* and *trans* diastereomers. Yield: 70%.

<sup>1</sup>H NMR (300 MHz, DMSO-*d*<sub>6</sub>, ppm)  $\delta$  = 8.63 (s, 1H, (**Z**)-**2**), 7.88 (s, 1H, (**E**)-**2**), 7.09 (d, *J* = 8.4 Hz, 2H, (**Z**)-**2**), 7.02 (d, *J* = 8.5 Hz, 2H, (**E**)-**2**), 6.66 (d, *J* = 8.4 Hz, 2H, (**Z**)-**2**), 5.74 (s, 1H), 2.47 – 2.32 (m, 1H), 2.12 – 1.50 (m, 8H). <sup>13</sup>C NMR (75 MHz, DMSO-*d*<sub>6</sub>)  $\delta$  = 28.86, 33.52, 39.52, 41.52, 61.90, 114.93, 127.71, 137.01, 156.44, 178.71: MS (ESI<sup>+</sup>): Calcd. for C<sub>14</sub>H<sub>16</sub>N<sub>2</sub>O<sub>3</sub>: 260.12, found: *m/z* 282.9 (M+Na)<sup>+</sup>, 261.0 (M+H)<sup>+</sup>.

### 2.2 Synthesis of 3,4,5-tris(decyloxy)benzoic anhydride (**3**)



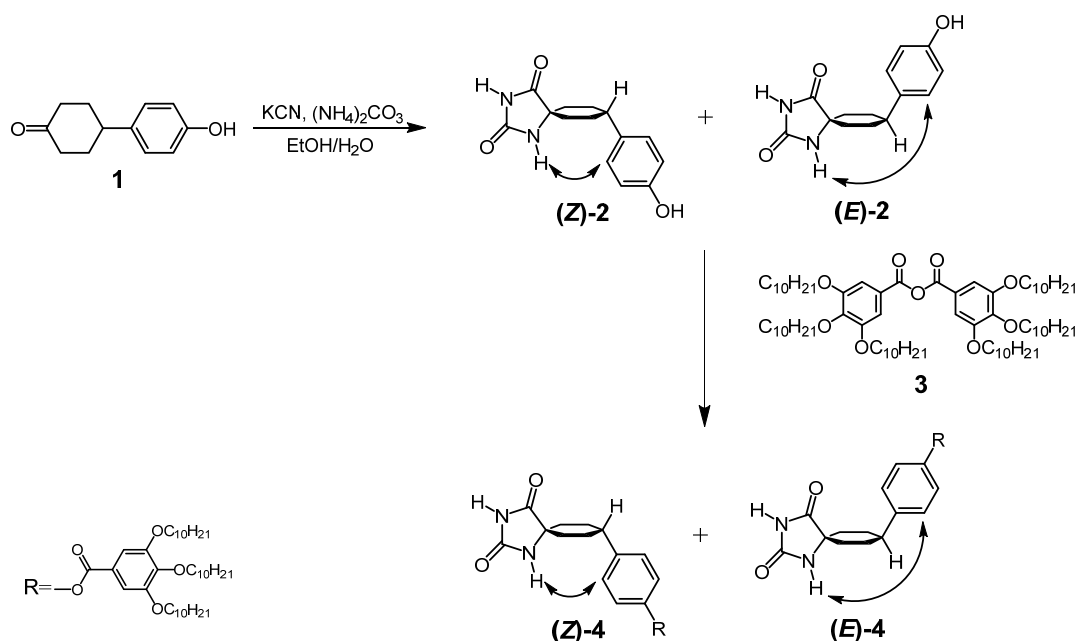
**Scheme S2.**

**Methyl 3,4,5-tris(decyloxy)benzoate.**<sup>2</sup> Methyl 3,4,5-trihydroxybenzoate (4.90 g, 26.61 mmol) and anhydrous potassium carbonate (13.00 g, 94.05 mmol) were stirred in 95 mL of dry DMF. The flask was heated to 100 °C under inert atmosphere and then 1-bromodecane (18.44 g, 83.38 mmol) was slowly added. The mixture was stirred at 100 °C overnight. Afterwards, it was allowed to cool to room temperature and an extraction was performed by adding water and solution of hexane/ethyl acetate (1:1) to the mixture. The organic layer was washed with NaOH (10%), washed with brine, dried over MgSO<sub>4</sub>, filtered and the solvent was evaporated. The resulting product was purified by column chromatography eluting with hexane/dichloromethane (3:2) to give a waxy product. Yield: 70%. <sup>1</sup>H NMR (300 MHz, CDCl<sub>3</sub>, ppm): δ = 7.27 (s, 2H), 4.08 – 3.98 (m, 6H), 3.91 (s, 3H), 1.84 – 1.74 (m, 6H), 1.48 – 1.28 (m, 42H), 0.95 – 0.84 (m, 9H). <sup>13</sup>C NMR (75 MHz, CDCl<sub>3</sub>): δ = 166.9, 152.8, 142.3, 124.8, 107.9, 73.5, 69.1, 52.0, 31.9, 30.3, 29.7-29.2, 26.0, 22.7, 14.1. MS (ESI<sup>+</sup>): Calcd. for C<sub>38</sub>H<sub>68</sub>O<sub>5</sub>: 604.5, found: m/z 627.5 (M+Na)<sup>+</sup>

**3,4,5-tris(decyloxy)benzoic acid.**<sup>2</sup> Methyl 3,4,5-tris(decyloxy)benzoate (9.11 g, 15.06 mmol) was dissolved in 1,4-dioxane (120 mL). The mixture was heated under reflux and then a solution of KOH (90%) (1.93 g, 34.42 mmol) in 1.6 mL of water was slowly added. The reaction mixture was stirred at reflux for 12 hours. After cooling to 0 °C, the mixture was acidified by slowly adding HCl (37%) until an acidic pH was attained. The precipitated product was filtered off and washed with water and ethanol. The obtained product was purified by recrystallization from glacial acetic acid, to give a white powder. Yield: 72%. <sup>1</sup>H NMR (400 MHz, CDCl<sub>3</sub>, ppm): δ = 7.27 (s, 2H), 4.04 (t, *J* = 6.7 Hz, 2H), 4.02 (t, *J* = 6.6 Hz, 4H), 1.82 – 1.73 (m, 6H), 1.51 – 1.20 (m, 42H), 0.88 (t, *J* = 7.0 Hz, 9H). <sup>13</sup>C NMR (100 MHz, CDCl<sub>3</sub>): δ = 172.2, 152.8, 143.0, 123.6, 108.4, 73.5, 69.1, 31.8, 30.8, 30.3, 29.7, 29.6, 29.5, 29.4, 29.3, 29.2, 26.0, 25.9, 22.6, 14.0. IR (KBr; cm<sup>-1</sup>): 2920, 2850, 1685, 1586, 1431, 1332, 1230, 1122. MS (ESI<sup>+</sup>): Calcd. for C<sub>37</sub>H<sub>66</sub>O<sub>5</sub>: 590.5, found: m/z 591.5 (M+H)<sup>+</sup>.

**3,4,5-tris(decyloxy)benzoic anhydride (3).**<sup>3</sup> Acetic anhydride (3.04 g, 29.8 mmol) and *p*-toluenesulfonic acid monohydrate (114 mg, 0.599 mmol) were added to a 50 mL toluene solution of 4.52 g (7.65 mmol) of 3,4,5-tris(decyloxy)benzoic acid, and the mixture was refluxed for 1 h. The excess acetic anhydride and generated acetic acid were removed by distillation. The crude product was purified by silica gel chromatography (ethyl acetate/*n*-hexane, 1:30) to give 3,4,5-tris(decyloxy)benzoic anhydride as a white solid. Yield: 62%. <sup>1</sup>H NMR (300 MHz, CDCl<sub>3</sub>, ppm) δ = 7.33 (s, 4H), 4.07 (t, *J* = 6.6 Hz, 4H), 4.01 (t, *J* = 6.4 Hz, 8H), 1.72-1.85 (m, 12H), 1.27-1.58 (m, 84H), 0.88 (t, *J* = 6.4 Hz, 18H). <sup>13</sup>C NMR (75 MHz, CDCl<sub>3</sub>) δ = 166.66, 152.93, 142.46, 125.22, 108.14, 73.64, 69.32, 65.31, 64.82, 53.56, 32.09, 32.07, 32.05, 30.48, 29.88, 29.82, 29.79, 29.74, 29.72, 29.70, 29.56, 29.51, 29.47, 29.45, 28.90, 26.25, 26.21, 26.19, 22.86, 22.84, 22.66, 14.26. MS (MALDI): Calcd. for C<sub>74</sub>H<sub>130</sub>O<sub>9</sub>: 1162.97, found: m/z 1186.0 (M+Na)<sup>+</sup>.

## 2.3 Synthesis of 4-(2,4-dioxo-1,3-diazaspiro[4.5]decan-8-yl)phenyl 3,4,5-tris(decyloxy) benzoate ((**Z**)-**4** and (**E**)-**4**)



**Scheme S3**

8-(4-Hydroxyphenyl)-1,3-diazaspiro[4.5]decan-2,4-dione (223 mg, 0.86 mmol) dissolved in DMF (2 mL) was added to 3,4,5-tris(decyloxy)benzoic anhydride (1g, 0.86 mmol) solution in DCM (2 mL). After 10 minutes DMAP (60 mg, 0.52 mmol) dissolved in 2 mL of DCM were added. The solution was stirred overnight at room temperature; afterwards 10 mL of hexane/AcOEt (1:1) were added. The organic layer was washed with brine, dried over MgSO<sub>4</sub>, filtered and the solvent was evaporated under vacuum. The mixture of diastereomers (**Z**)-**4** and (**E**)-**4** was purified and separated by silica gel chromatography (ethyl acetate/*n*-hexane, 2/3) to give two products. Yield: (**Z**)-**4**, 20% and (**E**)-**4**, 7%.

### (**Z**)-**4** diastereomer

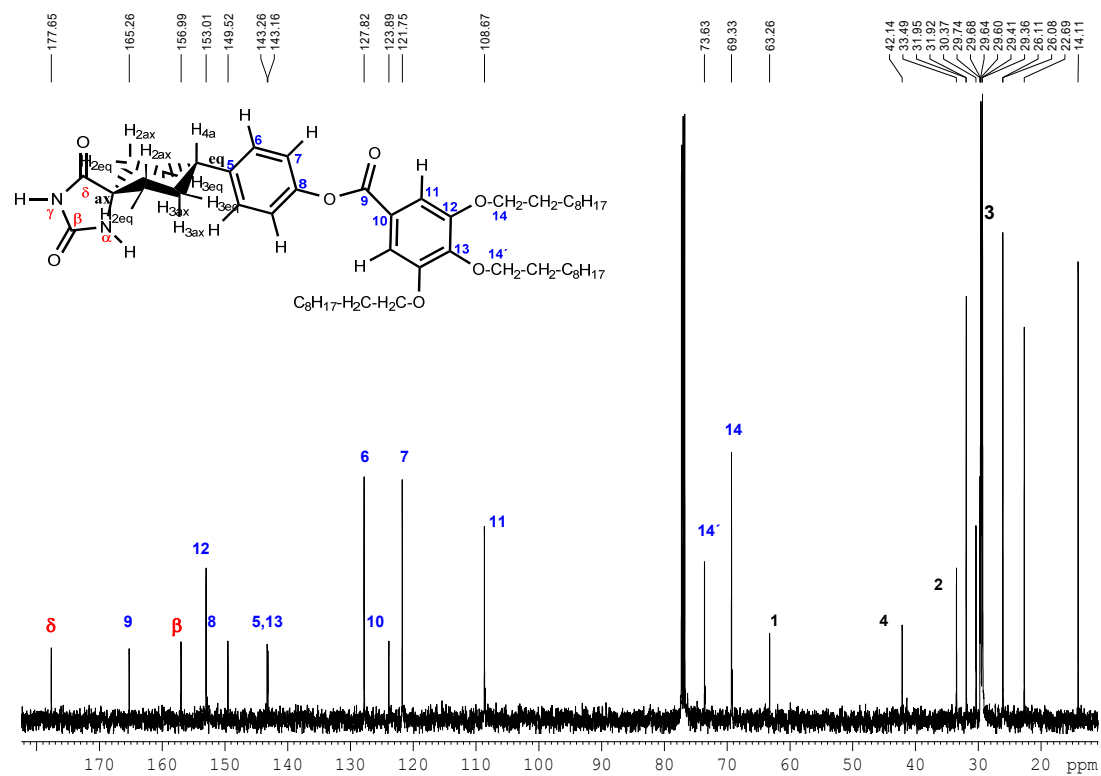
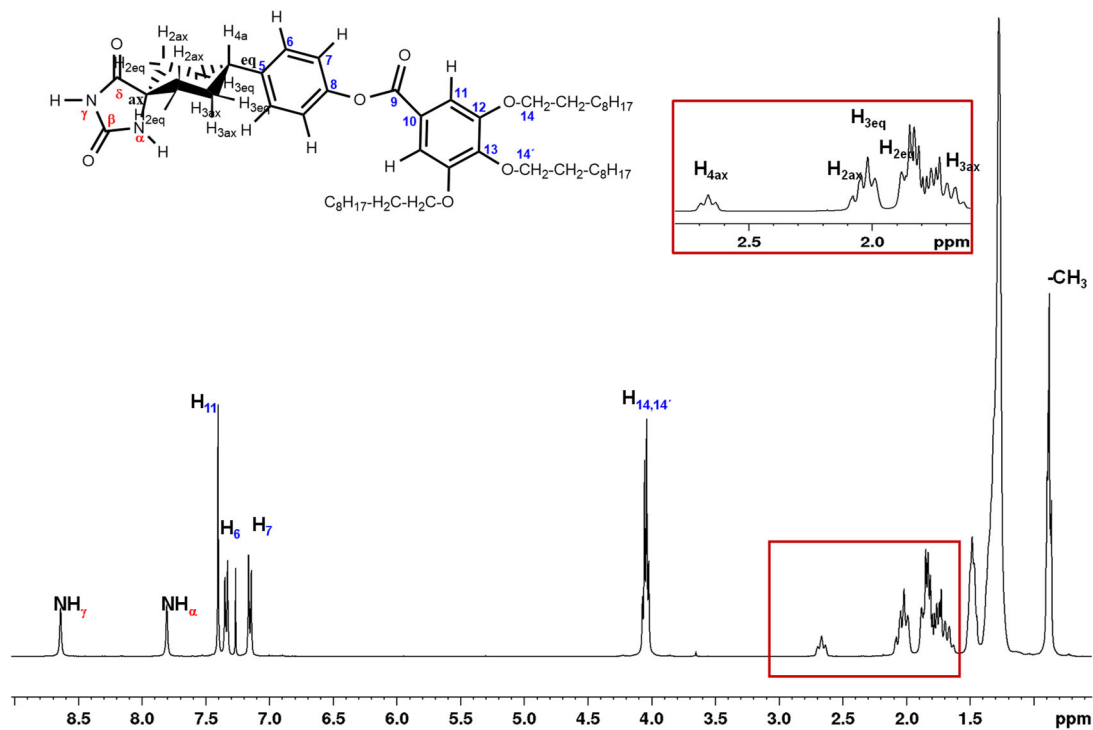
<sup>1</sup>H NMR (500 MHz, CDCl<sub>3</sub>) δ 8.65 (s, 1H), 7.81 (s, 1H), 7.40 (s, 2H), 7.37-7.29 (m, 2H), 7.20-7.10 (m, 2H), 4.14-3.94 (m, 6H), 2.74-2.59 (m, 1H), 2.13-1.93 (m, 4H), 1.93-1.58 (m, 10H), 1.57-1.42 (m, 6H), 1.41-1.17 (m, 36H), 0.94-0.81 (m, 9H). <sup>13</sup>C NMR (126 MHz, CDCl<sub>3</sub>) δ 177.65, 165.26, 156.99, 153.01, 149.42, 143.26, 143.16, 127.82, 123.89, 121.75, 108.67, 73.63, 69.33, 63.26, 42.14, 33.49, 31.95, 31.92, 30.37, 29.74, 29.68, 29.64, 29.60, 29.41, 29.36, 26.11, 26.08, 22.69, 14.11.

### (**E**)-**4** diastereomer

<sup>1</sup>H NMR (500 MHz, CD<sub>2</sub>Cl<sub>2</sub>) δ 7.75 (s, 1H), 7.39 (s, 2H), 7.37-7.31 (m, 2H), 7.15-7.10 (m, 2H), 5.38 (s, 1H), 4.01-3.98 (m, 6H), 2.62 (tt, *J* = 12.0, 3.5 Hz, 1H), 2.35-2.23 (m, 2H), 2.21-2.13 (m, 2H), 1.92-1.69 (m, 10H), 1.53-1.43 (m, 6H), 1.42-1.19 (m, 36H), 0.94-0.82 (m, 9H). <sup>13</sup>C NMR (126 MHz, CD<sub>2</sub>Cl<sub>2</sub>) δ 176.82, 165.52, 155.75, 153.42, 149.90, 144.12, 143.27, 128.28, 124.45, 122.08, 108.70, 73.92, 69.67, 61.35, 42.33, 35.39, 32.34, 30.76, 30.15, 30.09, 30.05, 30.00, 29.97, 29.81, 29.76, 29.61, 26.51, 26.48, 23.11, 14.28.

### 3. SUPPLEMENTARY FIGURES

#### 3.1. NMR Spectra



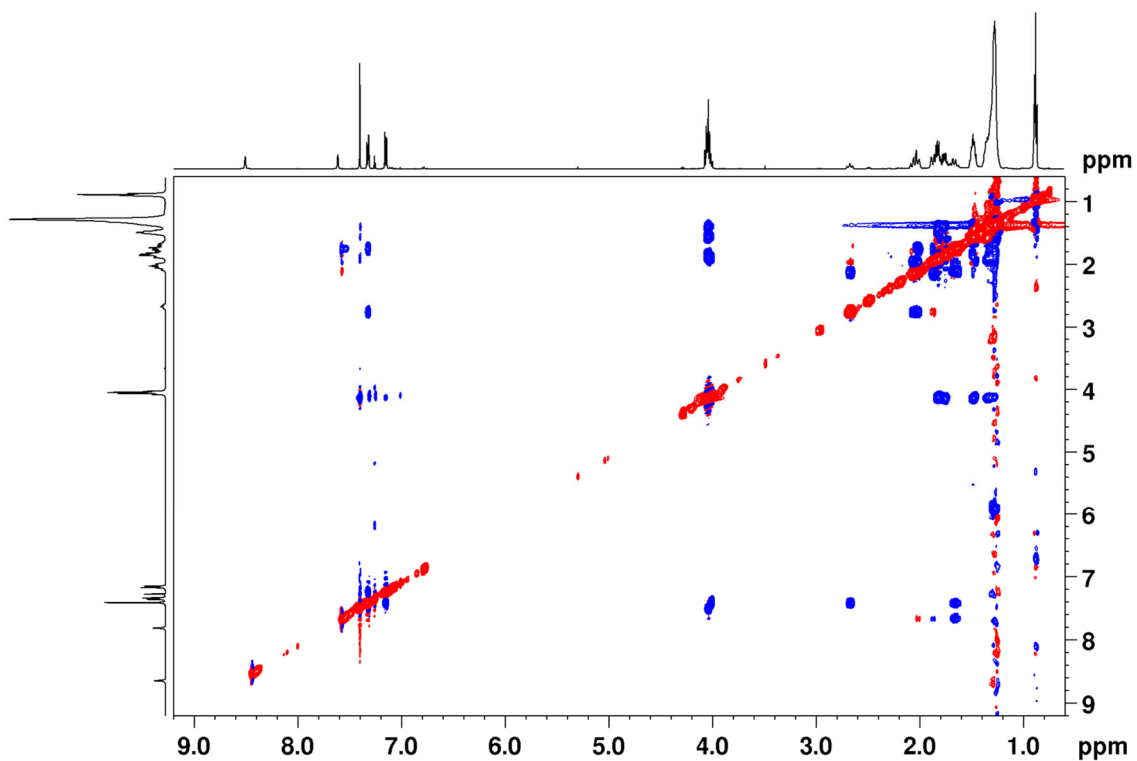


Figure S3.  $^1\text{H}$ - $^1\text{H}$  ROESY spectrum of *Z*-diastereomer (**Z**)-**4** (500 MHz, 298K,  $\text{CDCl}_3$ ).  $t_{\text{mix}}=400\text{ms}$ .

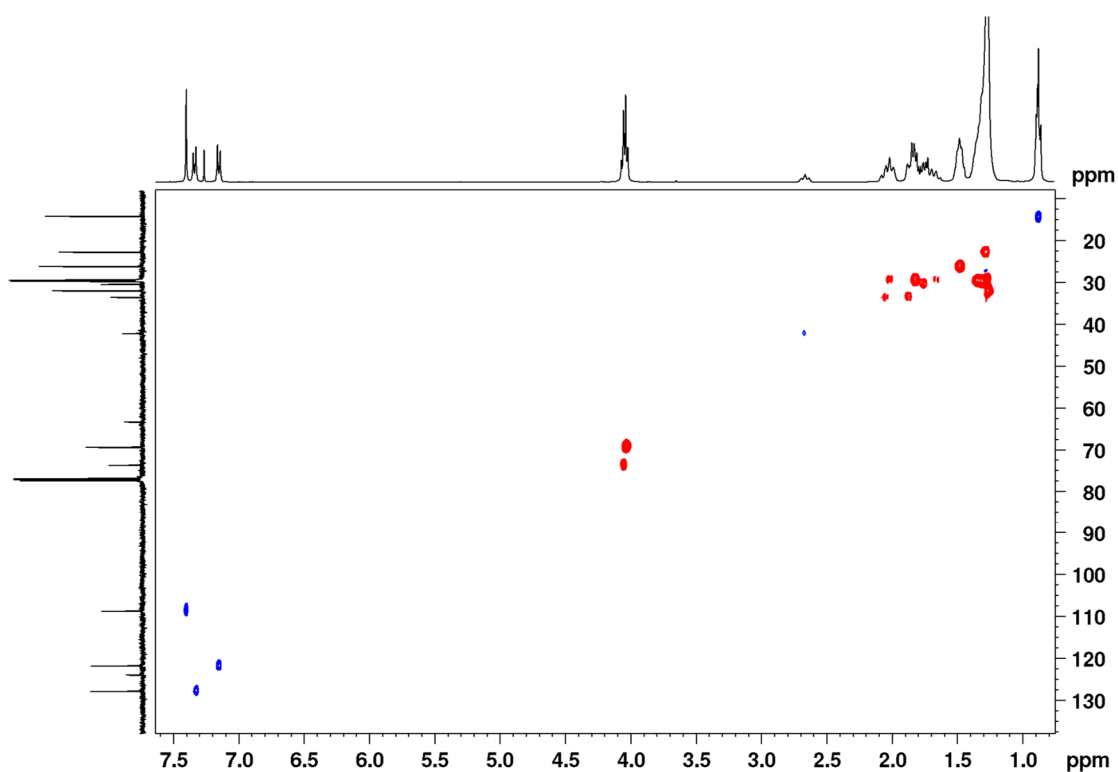


Figure S4.  $^1\text{H}$ - $^{13}\text{C}$  HSQC spectrum of *Z*-diastereomer (**Z**)-**4** (500 MHz, 298K,  $\text{CDCl}_3$ ).



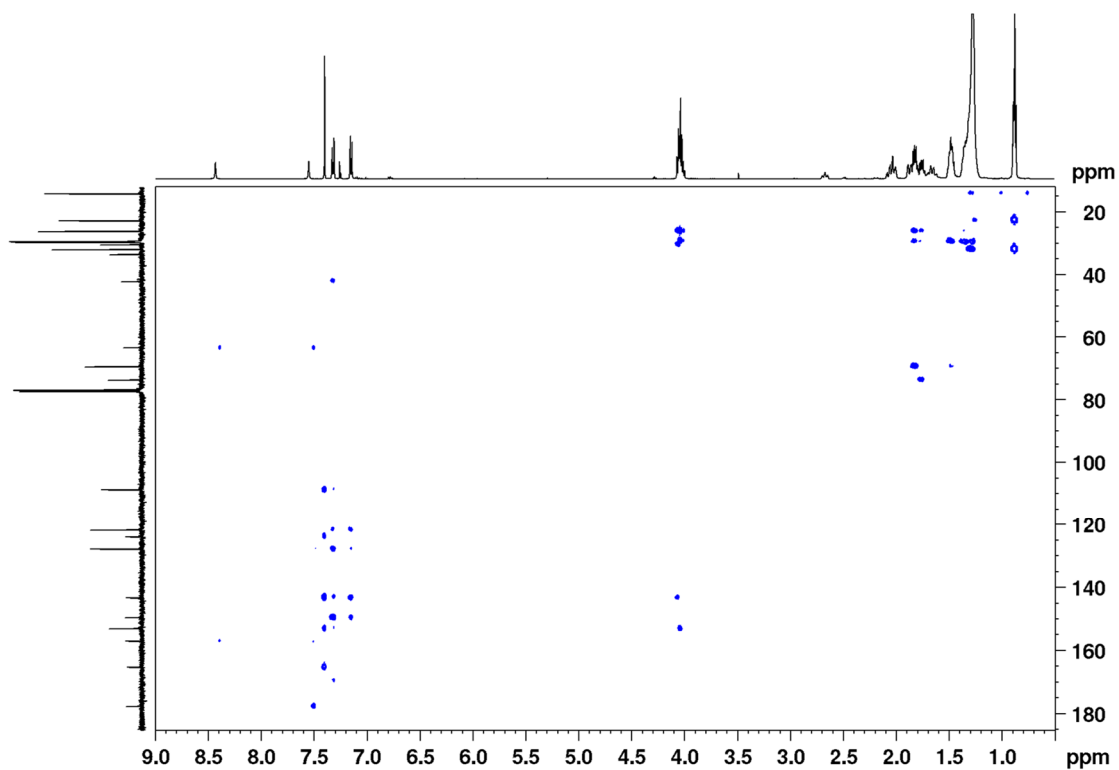


Figure S5.  $^1\text{H}$ - $^{13}\text{C}$  HMBC spectrum of *Z*-diastereomer (**Z**)-**4** (500 MHz, 298K,  $\text{CDCl}_3$ ).

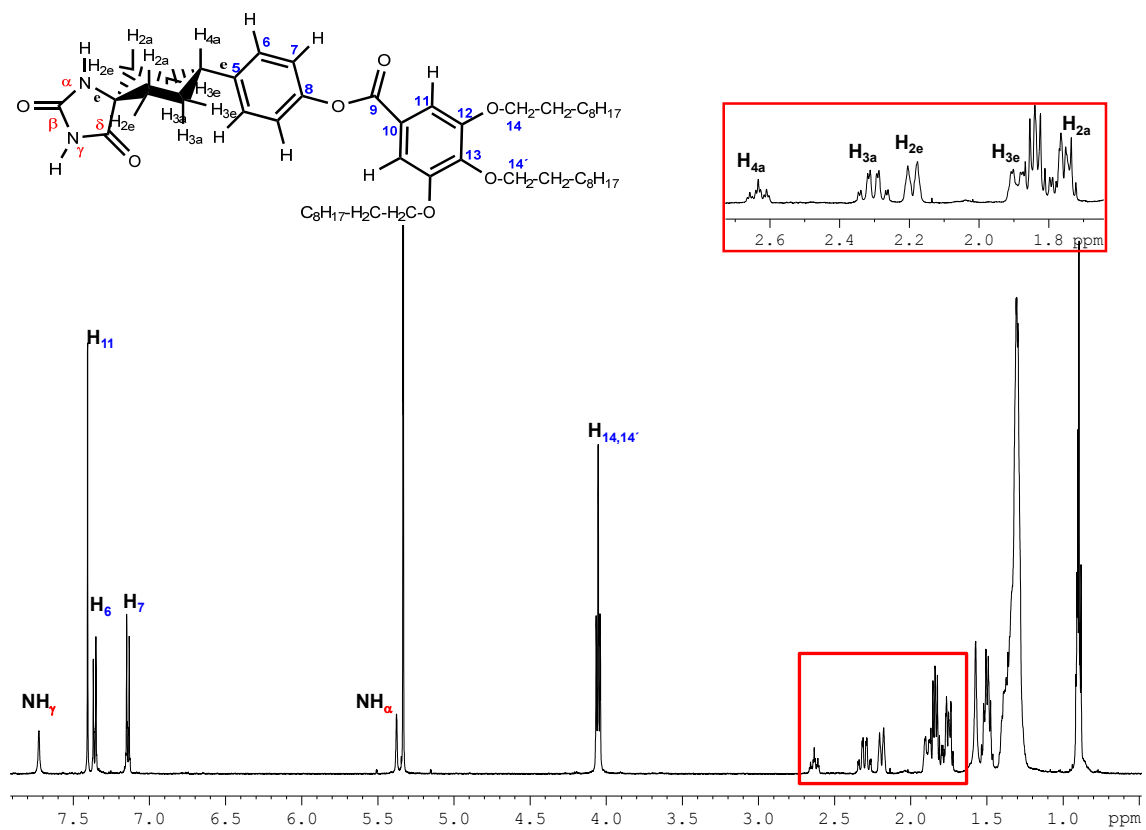


Figure S6.  $^1\text{H}$  NMR spectrum of *E*-diastereomer (**E**)-**4** (500 MHz, 298K,  $\text{CD}_2\text{Cl}_2$ ).

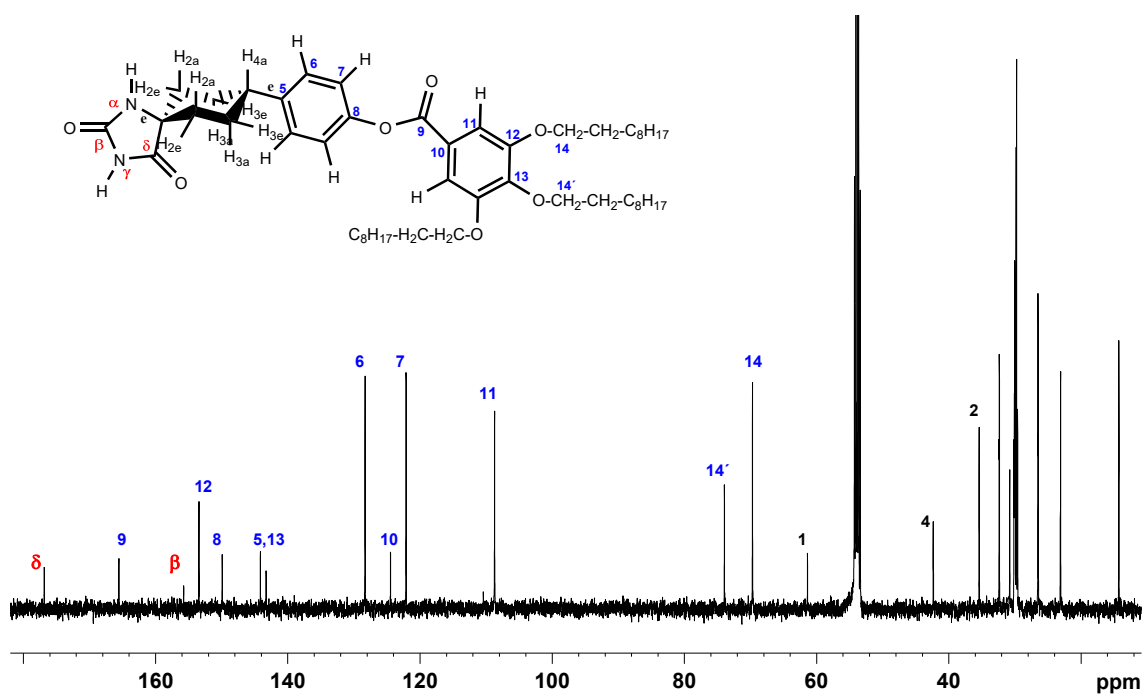


Figure S7.  $^{13}\text{C}$  NMR spectrum of *E*-diastereomer (*E*)-4 (125 MHz, 298K,  $\text{CD}_2\text{Cl}_2$ ).

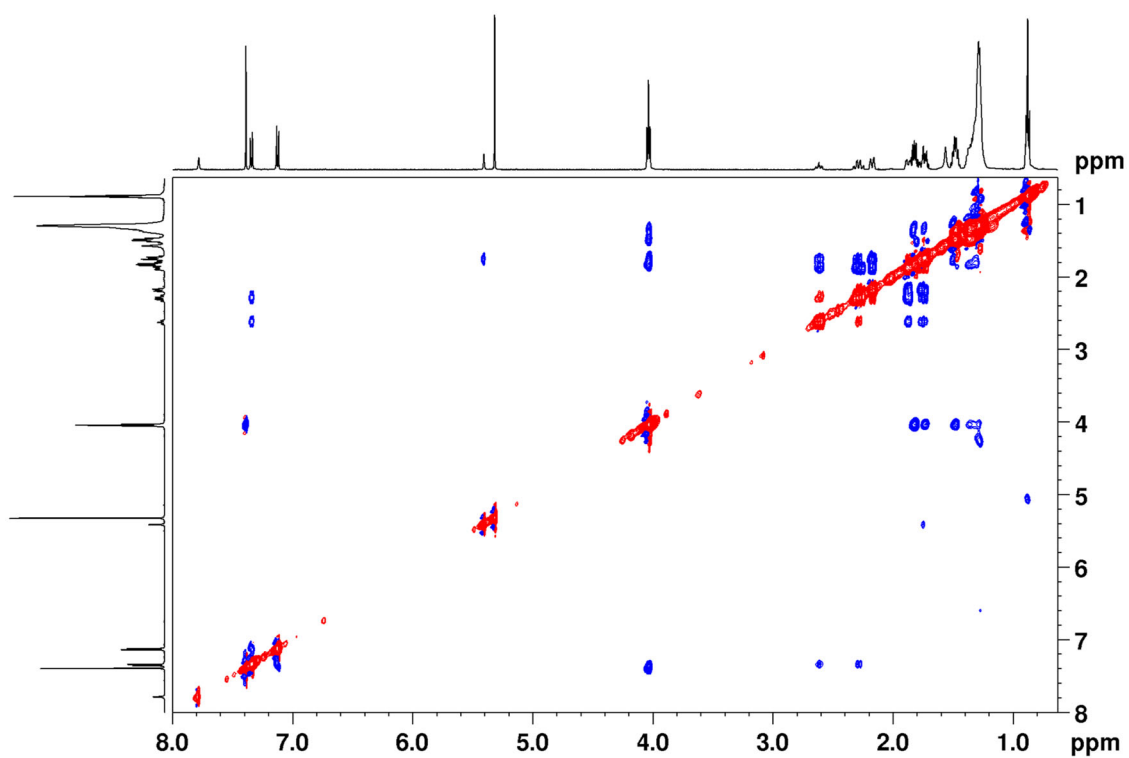


Figure S8.  $^1\text{H}$ - $^1\text{H}$  ROESY spectrum of *E*-diastereomer (*E*)-4 (500 MHz, 298K,  $\text{CD}_2\text{Cl}_2$ ).  
tmix=400ms.

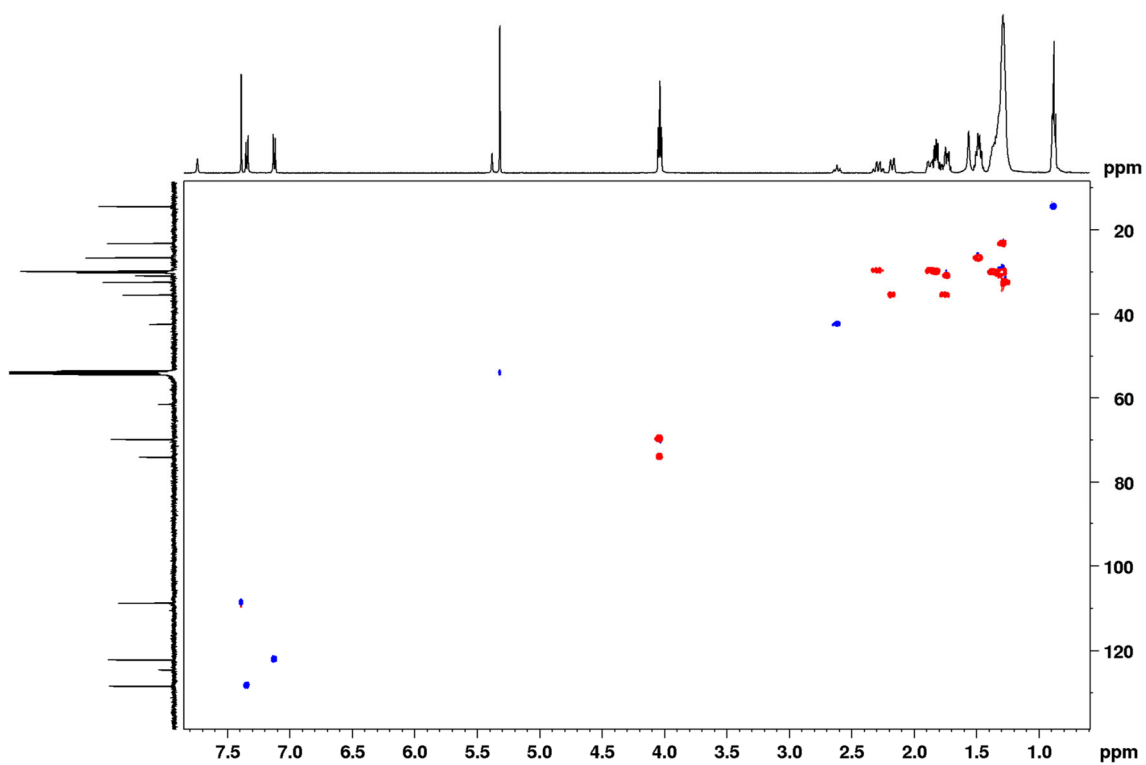


Figure S9.  $^1\text{H}$ - $^{13}\text{C}$  HSQC spectrum of *E*-diastereomer (*E*)-4 (500 MHz, 298K,  $\text{CD}_2\text{Cl}_2$ ).

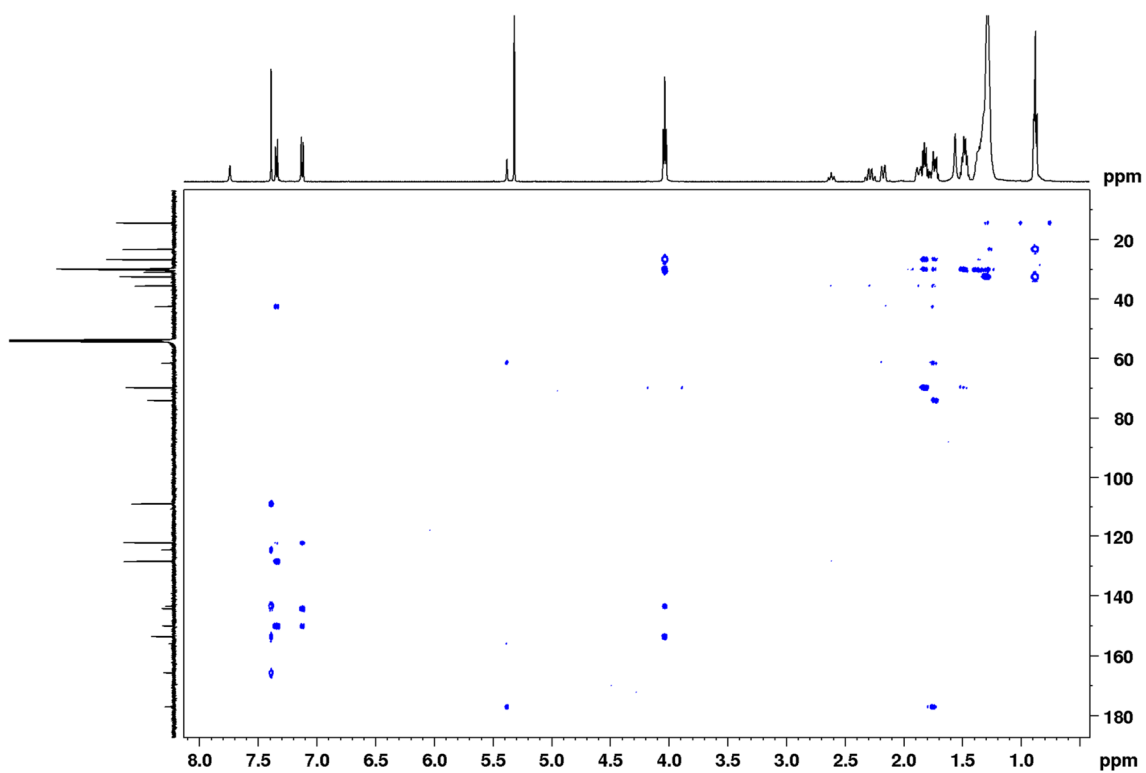


Figure S10.  $^1\text{H}$ - $^{13}\text{C}$  HMBC spectrum of *E*-diastereomer (*E*)-4 (500 MHz, 298K,  $\text{CD}_2\text{Cl}_2$ ).

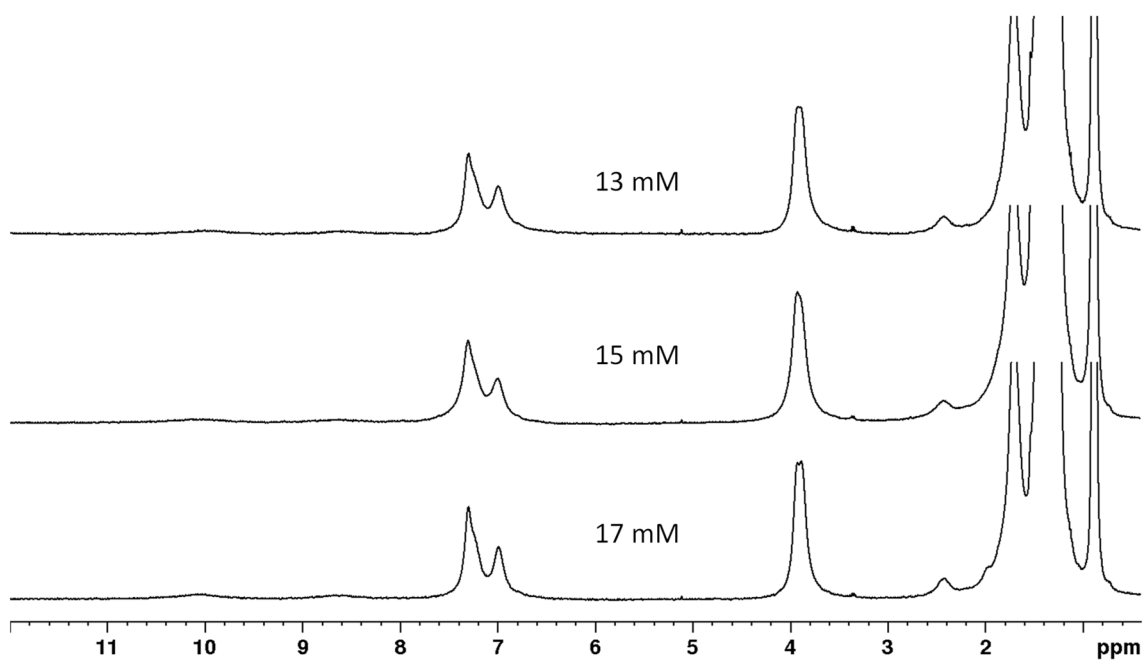


Figure S11. <sup>1</sup>H NMR spectra of Z-diastereomer (Z)-4 in C<sub>6</sub>D<sub>12</sub> at different concentrations.

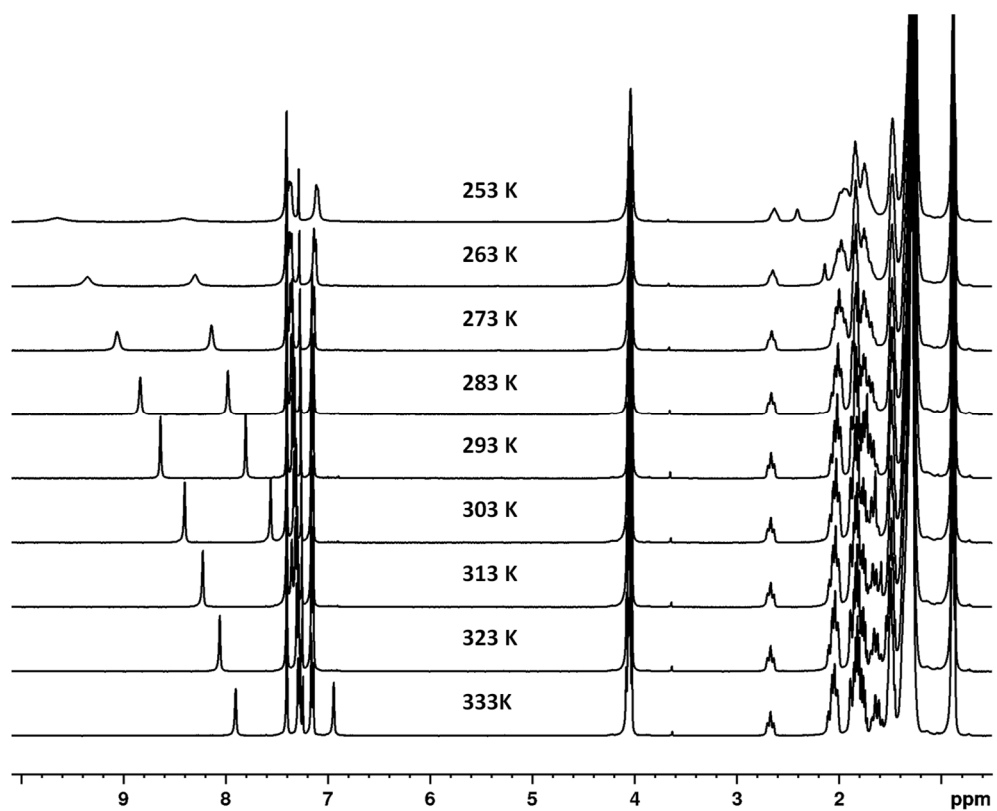
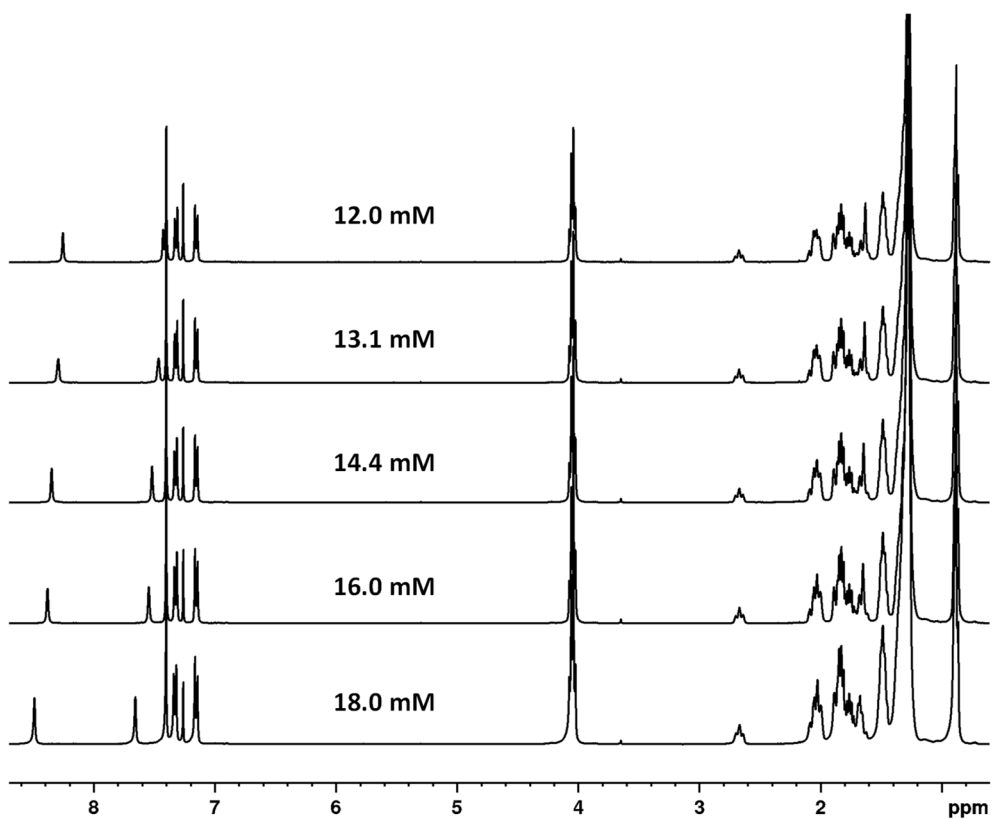
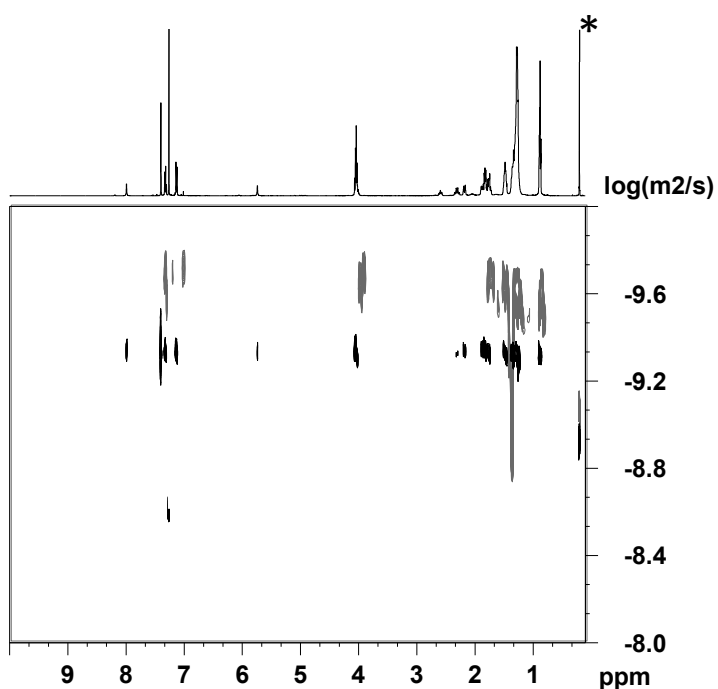


Figure S12. Temperature-dependent <sup>1</sup>H NMR spectra of (Z)-4 isomer at 16 mM in CDCl<sub>3</sub>.



**Figure S13.** Concentration-dependent  $^1\text{H}$  NMR spectra of (**Z**)-**4** isomer in  $\text{CDCl}_3$  at 298 K.



**Figure S14.**  $^1\text{H}$  DOSY NMR spectra of *E*-diastereomer (**E**)-**4** at 298 K in  $\text{CDCl}_3$  (bottom trace in black) and in a mixture 9:1  $\text{C}_6\text{D}_{12}:\text{CDCl}_3$  (top trace in gray). The projection is referenced to  $^1\text{H}$  in  $\text{CDCl}_3$  solution.

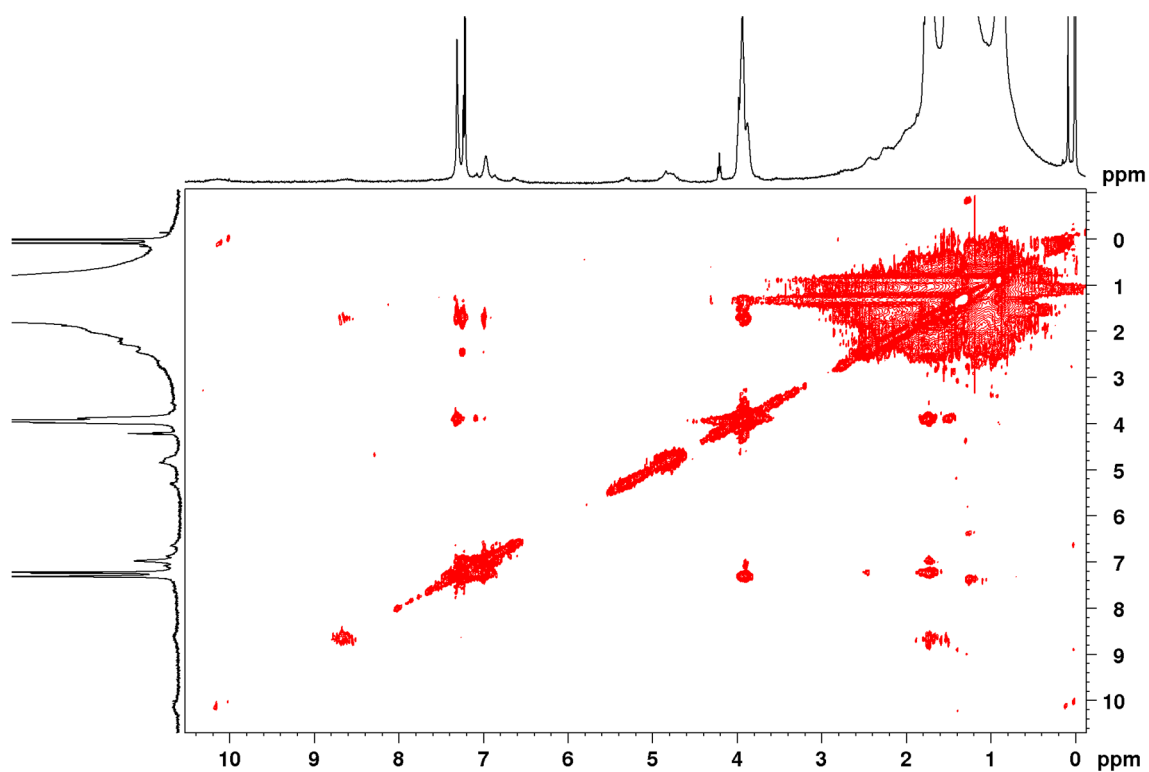


**Figure S15.** HRMAS  $^1\text{H}$  NOESY spectrum of Z-diastereomer (**Z**)-**4** (500 MHz, 298K,  $\text{C}_6\text{D}_6$ ). (tmix=40ms, spinning rate of 4 kHz).

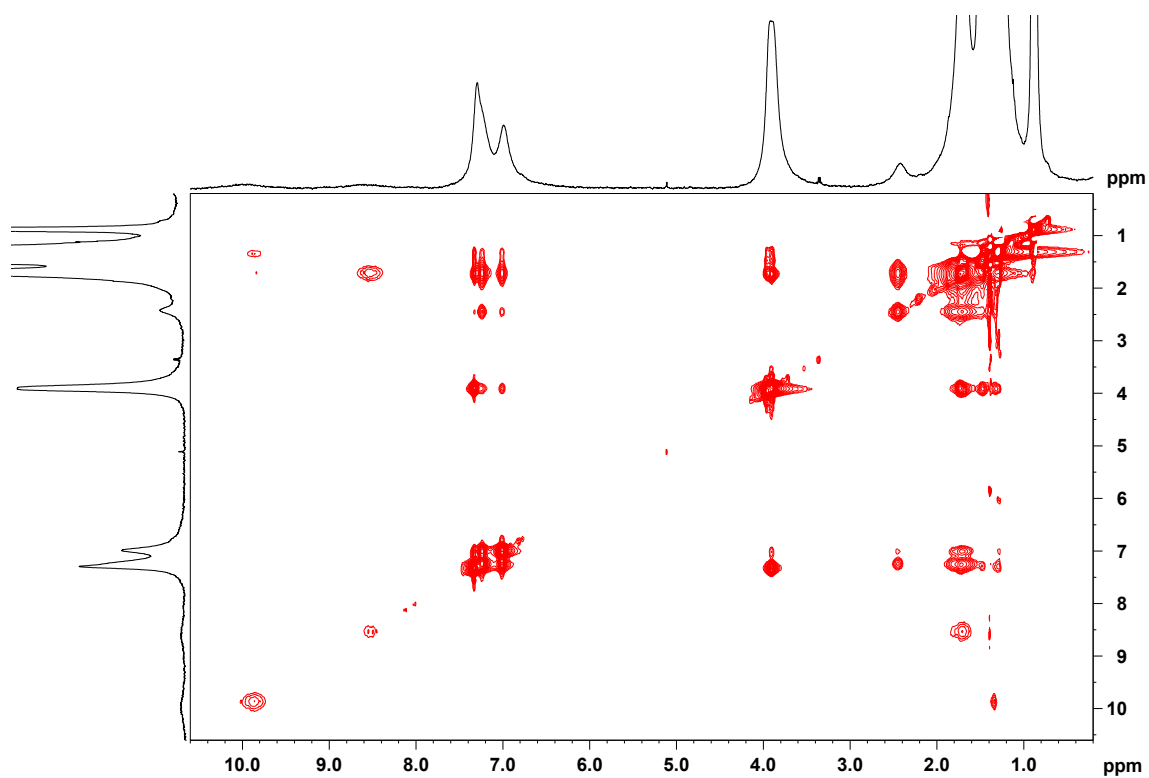


**Figure. 16.**  $^1\text{H}$ - $^1\text{H}$  NOESY spectrum of Z-diastereomer (**Z**)-**4** (500 MHz, 298K,  $\text{C}_6\text{D}_6$ ). tmix=400ms.

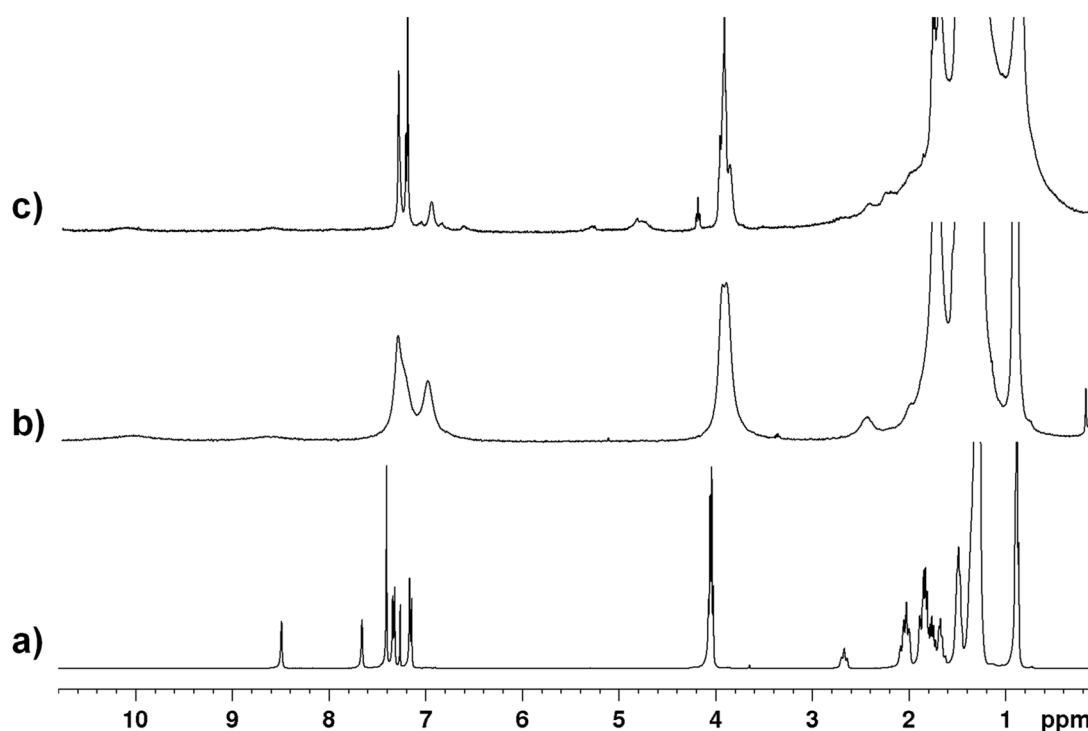


**Figure S17.**  $^1\text{H}$  NMR spectra of Z-diastereomer **(Z)-4** in solution: a) in  $\text{CDCl}_3$ , b) in  $\text{C}_6\text{D}_{12}$  and c) in gel phase in  $\text{C}_6\text{D}_{12}$  (MAS rotation 4 kHz).

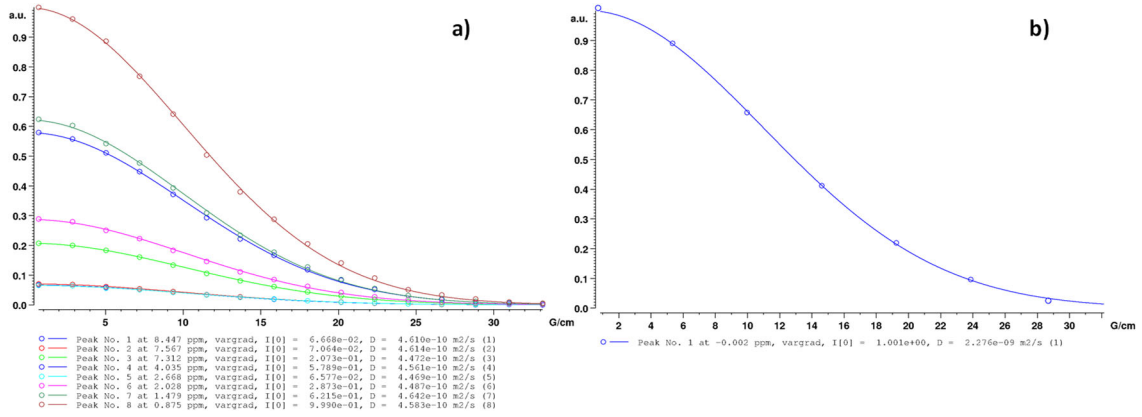
### **3.2. Quantitative DOSY analysis of diastereomer (Z)-4**

We have calculated the self-diffusion coefficients,  $D$ , from the modified Stejskal-Tanner equation:  $I = I_0 \exp[-D\gamma^2 G^2 \delta^2 (\Delta - \delta/3)]$ , where  $I$  and  $I_0$  are the resonance intensity measured for a gradient pulse or in his absence,  $\gamma$  is the gyromagnetic ratio of the hydrogen nucleus,  $G$  the pulse-gradient strength,  $\Delta$  is the diffusion time and  $\delta$  is the duration of the bipolar gradient pulse.

To circumvent changes of viscosity from one sample to another it is convenient by defining a reduced diffusion coefficient  $\Delta_{j(s)}$  (E. J. Cabrita and S. Berger, *Magn. Reson. Chem.*, 2001, 39, S142–S148.). We have used TMS as internal reference:  $\Delta_j = D_j / D_{\text{TMS}}$ . On the other hand, the ratio of diffusion coefficients for two different molecular species ( $D_i/D_j$ ) is inversely proportional to the square-root or to the cubic-root of the ratio of their molecular weights.

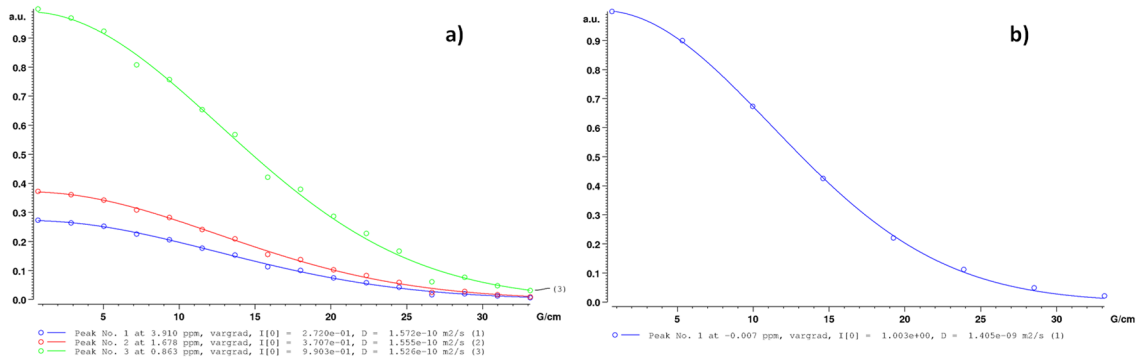
Two DOSY experiments have been carried out for each solvent:

In the case of dissolution in  $\text{CDCl}_3$ , the variation of resonance intensity with gradient intensity for a) **(Z)-4** ( $d_{20}=150\text{ms}$ ,  $p_{30}=1.6\text{ms}$ ) and b) TMS ( $d_{20}=100\text{ms}$ ,  $p_{30}=0.8\text{ms}$ ) are indicated below:



and its reduced diffusion coefficient:  $\Delta_{CDCl_3} = \frac{D_{(Z)-4}}{D_{TMS}} = \frac{4.55 \times 10^{-10}}{22.76 \times 10^{-10}} = 0.20$

In the case of dissolution in C<sub>6</sub>D<sub>12</sub>, the variation of resonance intensity with gradient intensity for a) (Z)-4 (d20=180ms, p30=2ms) and b) TMS (d20=100ms, p30=1ms) are:



and its reduced diffusion coefficient:  $\Delta_{C_6D_{12}} = \frac{D_{(Z)-4}}{D_{TMS}} = \frac{1.55 \times 10^{-10}}{14.05 \times 10^{-10}} = 0.11$

The ratio of diffusion coefficients for two different molecular species ( $D_i/D_j$ ) is inversely proportional to the square-root or to the cubic-root of the ratio of their molecular weights ( $M_j/M_i$ ) for rod-like and spherical molecules, respectively. Assuming that rosettes are hydrodynamically spherical, the average aggregate size can be estimated as  $N_{DOSY} = (M_{ag}/M) \approx (D/D_{ag})^3$ , In this case we use the reduced diffusion coefficients:

$$\frac{\Delta_{CDCl_3}}{\Delta_{C_6D_{12}}} = \frac{0.2}{0.11} = 1.81 \dots 1.81^3 \approx 5.96$$

which fits the proposal for the formation of a hexameric rosette for (Z)-4.



### 3.3. XRD

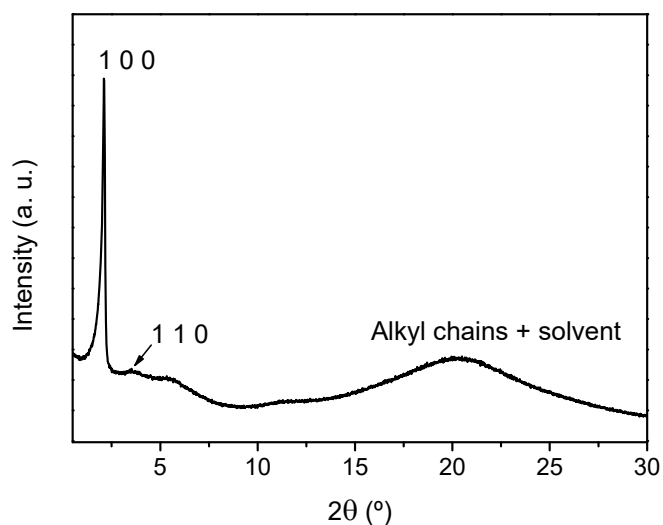


**Figure S18.** Room temperature XRD pattern of **(Z)-4** organogel in cyclohexane.

**Table S1.** X-Ray structural parameters of the mesophases of the pure compounds.

	$d_{\text{obs}}^{\text{a}}$ (Å)	$h k l^{\text{b}}$	Lattice parameters <sup>c</sup>
<b>(Z)-4</b>	42.2	1 0 0	$a = 48.4 \text{ Å}$
	23.9	1 1 0	$h = 4.1; Z = 6$
	4.4 (br)	Alkyl chains	
<b>(E)-4</b>	42.9	1 0 0	$a = 49.5 \text{ Å}$
	24.4	1 1 0	$h = 3.9; Z = 6$
	21.5	2 0 0	
	16.4	2 1 1	
	4.4 (br)	Alkyl chains	

<sup>a</sup>  $d_{\text{obs}}$ :  $d$  value calculated according to Bragg's equation.

<sup>b</sup> Miller indices.

<sup>c</sup>  $a$ : lattice constant of the columnar phase.  $a = (2/\sqrt{3}) \cdot (d_{10} + \sqrt{3} \cdot d_{11} + \sqrt{4} \cdot d_{20} + \sqrt{7} \cdot d_{21} + \dots) / n_{\text{reflections}}$

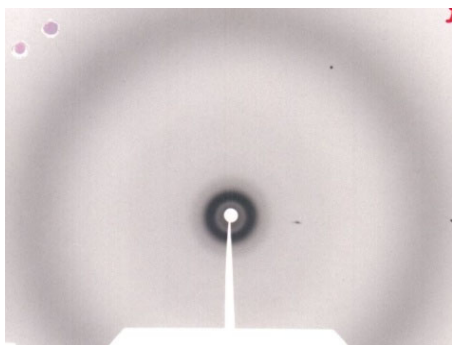


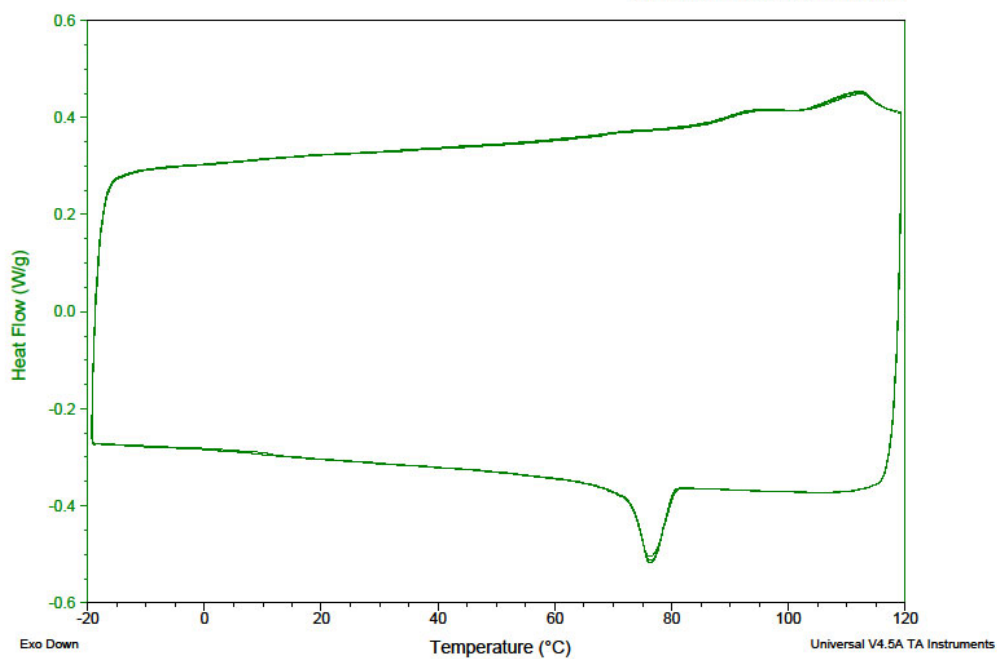
**Figure S19.** Room temperature XRD pattern of **(Z)-4** in the  $\text{Col}_h$  mesophase.

### 3.4.

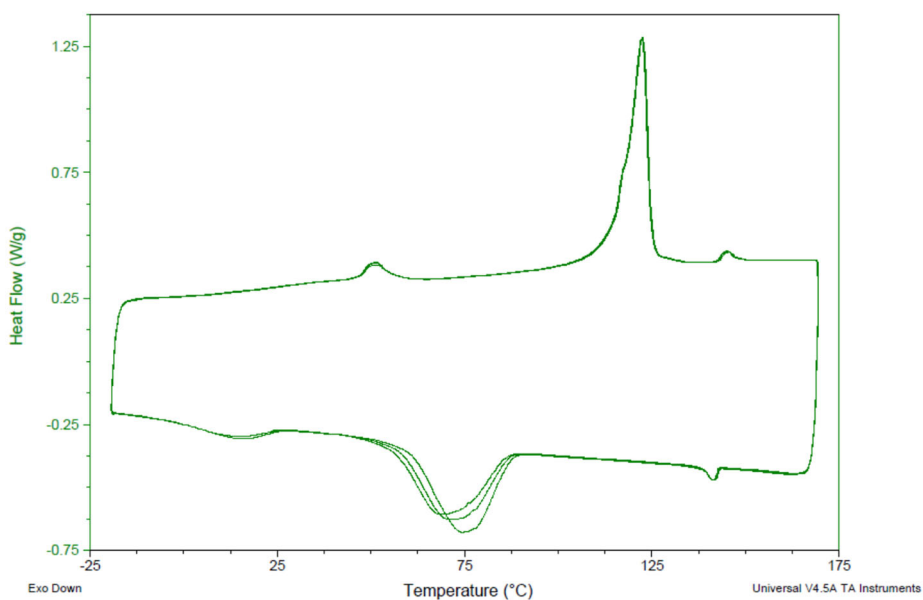
Sample: LG\_55\_dia1  
Size: 2.3470 mg

DSC

File: E:\LG\_55\_dia1  
Operator: Pedro  
Run Date: 08-Jul-2013 11:41  
Instrument: DSC Q20 V24.10 Build 122



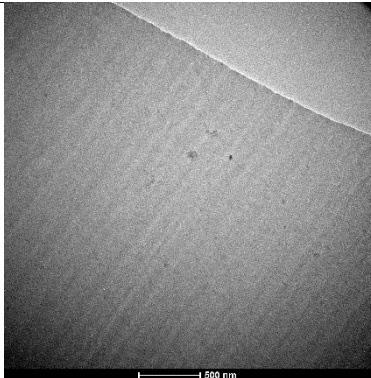
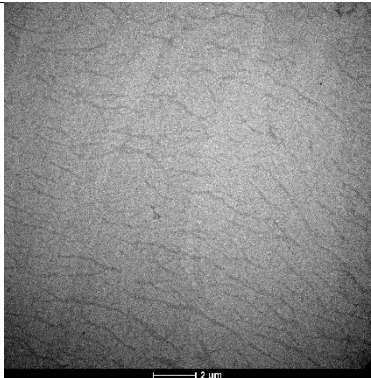
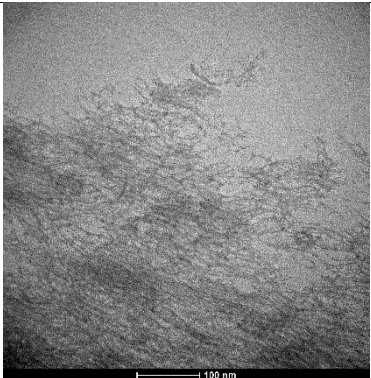
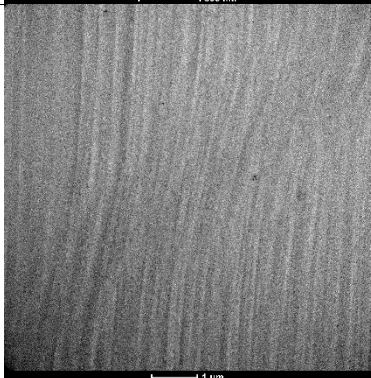
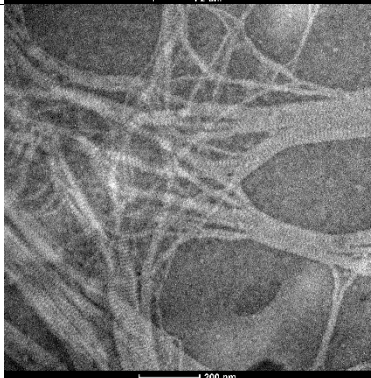
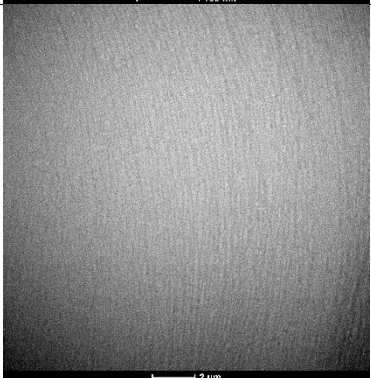
**Figure S20.** DSC traces corresponding to the second, third and fourth scans of compound **(Z)-4** (10°C/min).



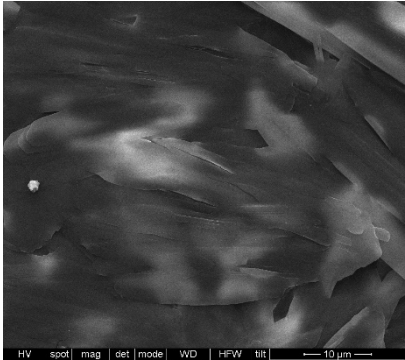
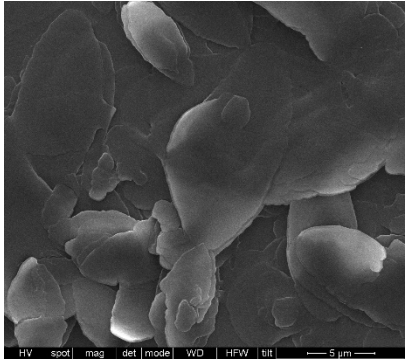
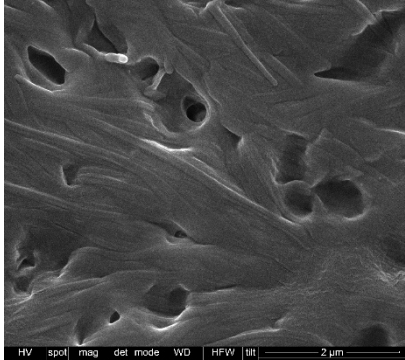
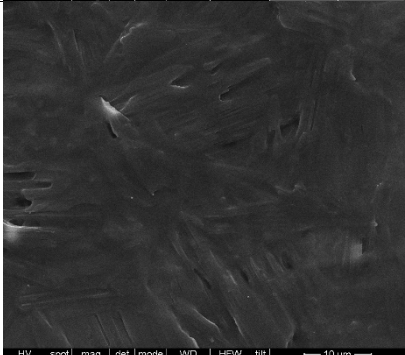
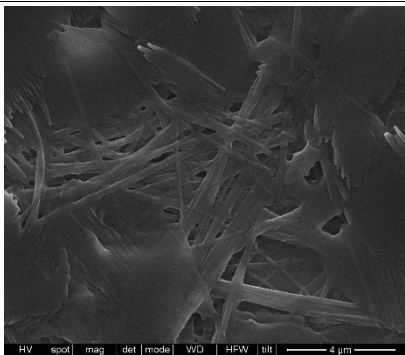
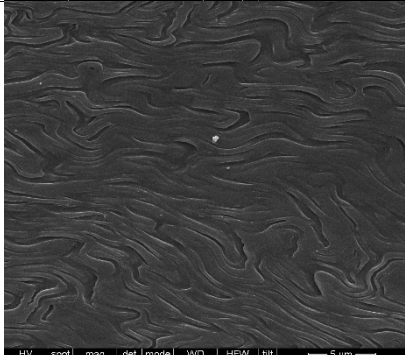
**Figure S21.** DSC traces corresponding to the second, third and fourth scans of compound **(E)-4** (10°C/min).

### 3.5. TEM and SEM images

**Table S2.** TEM microphotographs of Z-(4) in different solvents and concentrations.

	Dodecane	Heptane	Cyclohexane
1% wt.			
2% wt.			

**Table S3.** SEM microphotographs of Z-(4) in different solvents and concentrations.

	Dodecane	Heptane	Cyclohexane
1% wt.			
2% wt.			

## 4. Theoretical calculation

### 4.1. Computational details

Density functional theory (DFT) calculations were carried out by using Gaussian09 package.<sup>4</sup> DFT with the B3LYP exchange–correlation functional<sup>5–7</sup> and Grimme D3BJ dispersion correction scheme<sup>8,9</sup> was utilized in conjunction with the 6-31G\*\* basic set<sup>10</sup>. The interaction energies between of dimers and hexamers ( $\Delta E_{\text{int}}$ ) were calculated at the same level of theory as the difference between the total complex energy and the sum of the total energies of the hydantoin units. The interaction energies were corrected using the Boys–Bernardi counterpoise method in order to correct the basis set superposition error (BSSE)<sup>11</sup>.

NCI analysis was performed using Multiwfn software<sup>12</sup>. A density cutoff of  $\rho = 0.1$  au was applied. Three-dimensional plots were created taking an isovalue of 0.5 for the reduced density gradient (s) and coloring in the  $[-0.025, 0.025]$  a.u.  $\pm(\lambda^2)\rho$  range using VMD software<sup>13</sup>.

### 4.2. Results

**Table S4.** Interaction energies ( $\Delta E_{\text{int}}$  in  $\text{kJ mol}^{-1}$ ) calculated at the B3LYP-D3/6-31G\*\* level for dimers and hexamers of **(Z)-4-M** and **(E)-4-M**.

Complex	$\Delta E_{\text{int}}$ $\text{kJ mol}^{-1}$
<b>(Z)-4-M DIMER</b>	-77.0
<b>(E)-4-M DIMER</b>	-66.3
<b>(Z)-4-M HEXAMER</b>	-444.9
<b>(E)-4-M HEXAMER</b>	-317.5

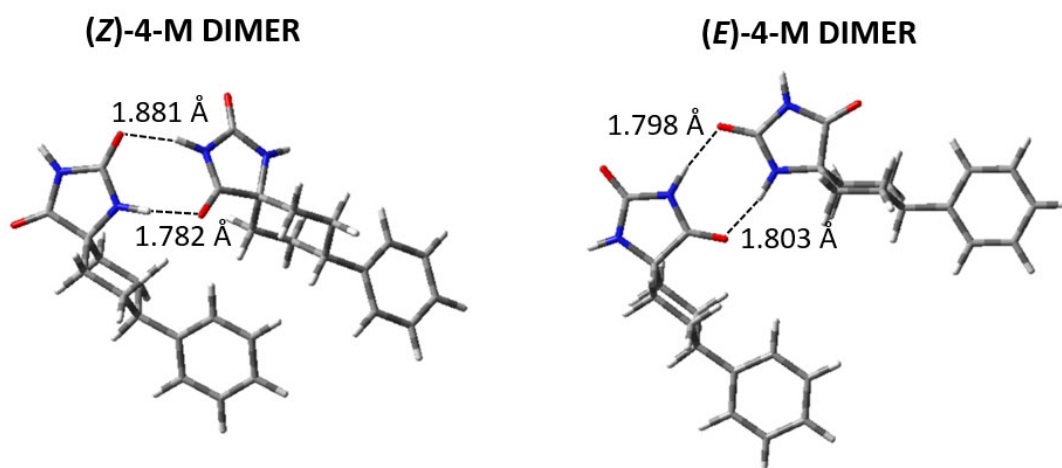


**Figure S22.** B3LYP-D3/6-31G\*\* optimized structures calculated for **(Z)-4-M** and **(E)-4-M** with hydrogen bond distances.

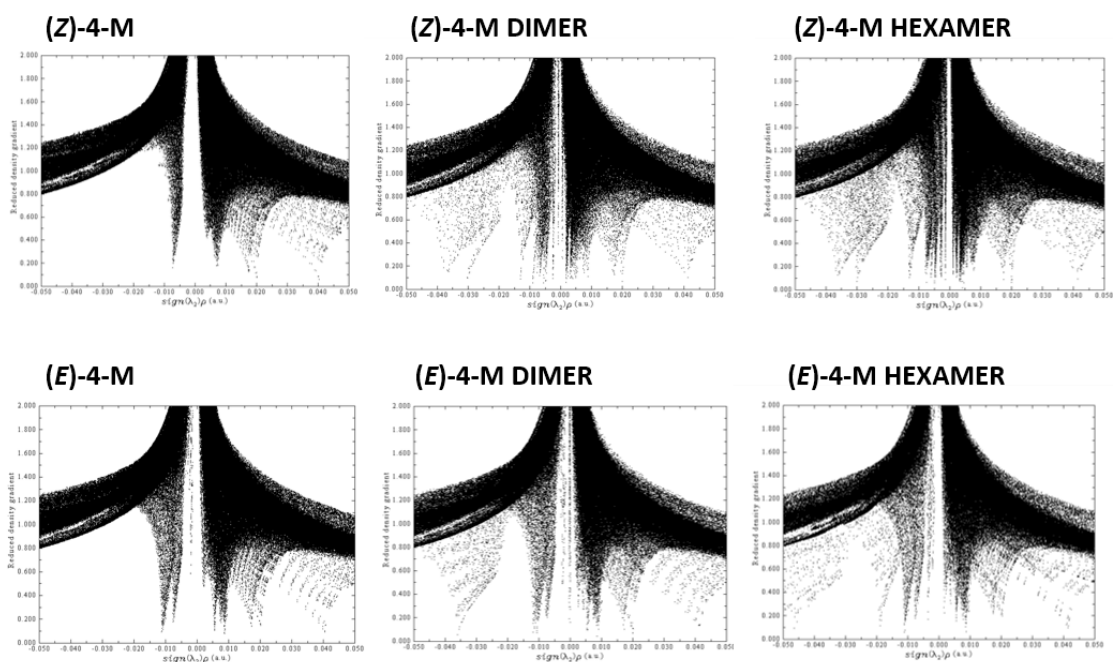


Figure S23. NCI plots of models, dimers and hexamers.

## 5. References

- 1 S. Graus, S. Uriel and J. L. Serrano, Supramolecular hydrogen-bonding patterns in 4'-substituted cyclohexane-5-spirohydantoin, *CrystEngComm*, 2012, **14**, 3759–3766.
- 2 J. Barbera, L. Puig, P. Romero, J. L. Serrano and T. Sierra, Propeller-like hydrogen-bonded banana-melamine complexes inducing helical supramolecular organizations, *J. Am. Chem. Soc.*, 2006, **128**, 4487–4492.
- 3 K. Kishikawa, S. Furusawa, T. Yamaki, S. Kohmoto, M. Yamamoto and K. Yamaguchi, Novel superstructure of nondiscoid mesogens: Uneven-parallel association of half-disk molecules, 3,4,5-trialkoxybenzoic anhydrides, to a columnar structure and its one-directionally geared interdigitation, *J. Am. Chem. Soc.*, 2002, **124**, 1597–1605.
- 4 M. J. Frisch, G. W. Trucks, H. B. Schlegel, G. E. Scuseria, M. A. Robb, J. R. Cheeseman, G. Scalmani, V. Barone, G. A. Petersson, H. Nakatsuji, X. Li, M. Caricato, A. Marenich, J. Bloino, B. G. Janesko, R. Gomperts, B. Mennucci, H. P. Hratchian, J. V. Ortiz, A. F. Izmaylov, J. L. Sonnenberg, D. Williams-Young, F. Ding, F. Lipparini, F. Egidi, J. Goings, B. Peng, A. Petrone, T. Henderson, D. Ranasinghe, V. G. Zakrzewski, J. Gao, N. Rega, G. Zheng, W. Liang, M. Hada, M. Ehara, K. Toyota, R. Fukuda, J. Hasegawa, M. Ishida, T. Nakajima, Y. Honda, O. Kitao, H. Nakai, T. Vreven, K. Throssell, J. J. A. Montgomery, J. E. Peralta, F. Ogliaro, M. Bearpark, J. J. Heyd, E. Brothers, K. N. Kudin, V. N. Staroverov, T. Keith, R. Kobayashi, J. Normand, K. Raghavachari, A. Rendell, J. C. Burant, S. S. Iyengar, J. Tomasi, M. Cossi, J. M. Millam, M. Klene, C. Adamo, R. Cammi, J. W. Ochtersk, R. L. Martin, K. Morokuma, O. Farkas, J. B. Foresman and D. J. Fox, *Gaussian 09, Revision A.02*, Gaussian Inc., Wallinford, CT, 2016.

- 5 C. T. Lee, W. T. Yang and R. G. Parr, Development of the colle-salvetti correlation-energy formula into a functional of the electron-density, *Phys. Rev. B*, 1988, **37**, 785–789.
- 6 A. D. Becke, C. T. Lee, W. T. Yang, R. G. Parr and A. D. Becke, Density-functional thermochemistry .3. The role of exact exchange, *J. Chem. Phys.*, 1993, **98**, 5648–5652.
- 7 A. D. Becke, A new mixing of hartree-fock and local density-functional theories, *J. Chem. Phys.*, 1993, **98**, 1372–1377.
- 8 H. Grimme, S.; Antony, J.; Ehrlich, S.; Krieg, S. Grimme, J. Antony, S. Ehrlich and H. Krieg, A consistent and accurate ab initio parametrization of density functional dispersion correction (DFT-D) for the 94 elements H-Pu, *J. Chem. Phys.*, 2010, **132**, 154102.
- 9 S. Grimme, S. Ehrlich and L. Goerigk, Effect of the damping function in dispersion corrected density functional theory, *J. Comput. Chem.*, 2011, **32**, 1450–1495.
- 10 M. M. Francl, W. J. Pietro, W. J. Hehre, J. S. Binkley, M. S. Gordon, D. J. DeFrees and J. A. Pople, Self-consistent molecular orbital methods. XXIII. A polarization-type basis set for second-row elements, *J. Chem. Phys.*, 1982, **77**, 3654–3665.
- 11 S. F. Boys and F. Bernardi, Calculation of small molecular interaction by differences of separate total energies -Some procedures with reduced errors, *Mol. Phys.*, 1970, **19**, 553–566.
- 12 T. Lu and F. Chen, Multiwfn: A multifunctional wavefunction analyzer, *J. Comput. Chem.*, 2012, **33**, 580–592.
- 13 W. Humphrey, A. Dalke and K. Schulten, VMD: Visual molecular dynamics, *J. Mol. Graph. Model.*, 1996, **14**, 33–38.